

Special Issue of the 8th International Advances in Applied Physics and Materials Science Congress (APMAS 2018)

Effects of Plasma Ion Nitriding Temperatures on Cavitation-Erosion Resistance of STS 304 in Seawater

S.O. CHONG^a AND S.J. KIM^{b, *}^aDNV GL, Division of Maritime, Busan, 46971, Rep. of Korea^bMokpo Maritime University, Division of Marine Engineering, Mokpo, 58628, Rep. of Korea

Plasma ion nitridation was performed on stainless steel at various temperature parameters to characterize cavitation-erosion resistance under seawater conditions. Plasma ion nitriding was carried out at a relatively low temperature of 400 to 500 °C for 10 h at a gas ratio of 25% N₂ + 75% H₂ and a chamber pressure of 250 Pa in consideration of corrosion resistance by chlorine ions. Cavitation-erosion experiments were conducted for 10 h in compliance with modified ASTM G-32. The cavitation-erosion test for 10 h showed the lowest surface damage, weight loss, and depth of damage at 450 °C, where the γ_N phase was most deeply formed. On the other hand, at 500 °C, the cavitation-erosion damage tended to increase with increasing γ' -Fe₄N phase and CrN.

DOI: [10.12693/APhysPolA.135.968](https://doi.org/10.12693/APhysPolA.135.968)

PACS/topics: plasma, stainless steel, cavitation-erosion, seawater, corrosion resistance

1. Introduction

Cavitation-erosion causes damage on the surface of the material due to the simultaneous action of the shock wave caused by bubble collapse and micro-jet generated when bubble collapse [1]. Plasma ion nitriding technology, which is a thermochemical surface treatment method, is widely used to improve the mechanical properties of stainless steel [2, 3]. Especially, when plasma ion nitridation treatment is performed at low temperature, the corrosion resistance is improved by the formation of expanded austenite (S-phase) [4]. However, when stainless steel is used under seawater environment, physical damage due to cavity impact pressure and electrochemical damage due to chlorine ion are superimposed to accelerate damage [5]. Espitia and Allenstein et al. have studied cavitation-erosion resistance in aqueous solutions and artificial chloride solutions after plasma ion nitriding for stainless steels [6, 7], but little research has been done in seawater solutions. Gallagher and Chong described electrochemical corrosion properties of plasma ion nitrided stainless steels depending on the medium in natural seawater and NaCl and HCl [8, 9]. Therefore, in this study, plasma ion nitriding process was applied to stainless steel at low temperatures in consideration of corrosion resistance under seawater environment, and cavitation-erosion resistance characteristics with temperature variables were investigated.

2. Experimental procedure

The chemical composition (wt%) of 304 stainless steel (STS 304) used in this study is 0.062C, 0.434Si, 1.101Mn, 0.0032S, 18.16Cr, 8.08Ni, 0.418Cu, 0.14Mo and

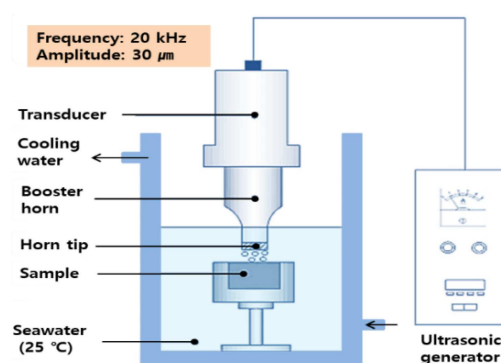


Fig. 1. Schematic diagram of cavitation-erosion experiment.

Fe-balance. Plasma ion nitridation was carried out at the conditions of a gas ratio of 25% N₂ and 75% H₂, at a chamber pressure of 250 Pa and at a temperature of 400–500 °C for 10 h. Figure 1 shows a schematic diagram of a cavitation-erosion experiment. The cavitation-erosion experiments were performed by applying the opposite vibration method at frequencies of 20 kHz and amplitudes of 30 μm in accordance with modified ASTM G-32 specification [10]. Cavitation-erosion experiments were carried out by applying a cavity impact pressure to the surface of the material for 1 to 10 h, while maintaining the seawater temperature at 25 °C and the distance between the horn tip and the surface of the specimen at 1 mm. After the plasma ion nitridation process, X-ray diffraction analysis was performed to analyze the phase change formed on the nitrided layer surface with the process temperature. The Vickers hardness of the material surface was measured to verify the change of mechanical properties under the conditions of an applied load of 9.807 N and a duration of 10 seconds. The cavitation-erosion resistance characteristics were analyzed with process temperature and cavitation-erosion time parameters by measuring the depth of damage, weight loss and surface damage observation with a 3D microscope.

*corresponding author; e-mail: ksj@mmu.ac.kr

3. Results and discussion

Figure 2 shows the cross-sectional micrographs of the specimen after etching in 30% HNO₃ + 50% HCl + 20% H₂O solution and measured the nitrided layer depth and surface hardness. The thickness of the nitrided layer increased as the temperature increases due to the increase of diffusion coefficient of nitrogen. The thickness of the nitrided layer was gently increased from 400 °C (Fig. 2b) to 450 °C (Fig. 2c) other than 500 °C (Fig. 2d) that dramatically increased due to the exponential increase in nitrogen diffusion [11]. The value of surface hardness also increased with increasing temperatures, and it was 4.1 times higher at 500 °C (Fig. 2d) than the untreated material (Fig. 2a). Stainless steel has a higher affinity in nitrogen than other elements, so that internal penetration of nitrogen easily diffuses with increasing temperatures, whereby increasing of the surface hardness of the uppermost layer [12].

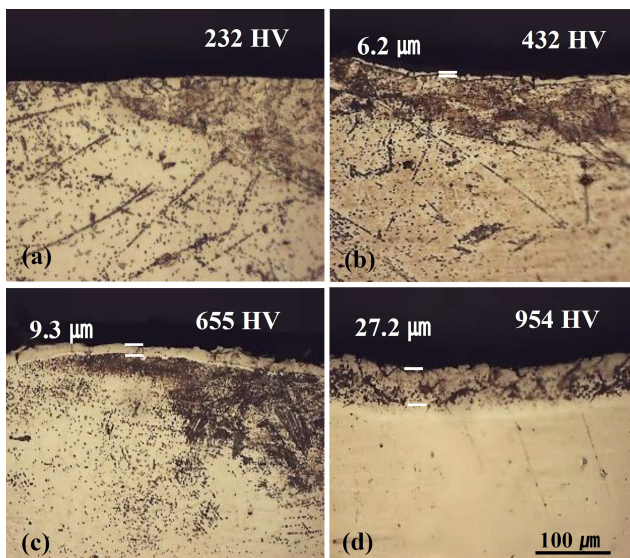


Fig. 2. Cross-sectional micrographs of the untreated and plasma ion nitrided STS 304 specimen (a) untreated, (b) 400 °C, (c) 450 °C, (d) 500 °C.

Figure 3 presents the results of X-ray diffraction analysis. The γ_N phase (S-phase) was observed in all plasma ion nitrided specimens. The angle γ_N phase until 450 °C was shifted to lower and the peak was to be high and sharpened with increasing temperature so that nitrogen supersaturated solid layer deepens [13]. In addition, at 500 °C, γ' -Fe₄N phase increases the hardness and CrN, which causes sensitization due to the formation of chromium depletion region in stainless steel, were formed [14]. Thus, an increase in hardness was observed due to the formation of γ' -Fe₄N phase at 500 °C, and it was confirmed in Fig. 2 that it turned dark because of CrN by the corrosion reaction during the etching.

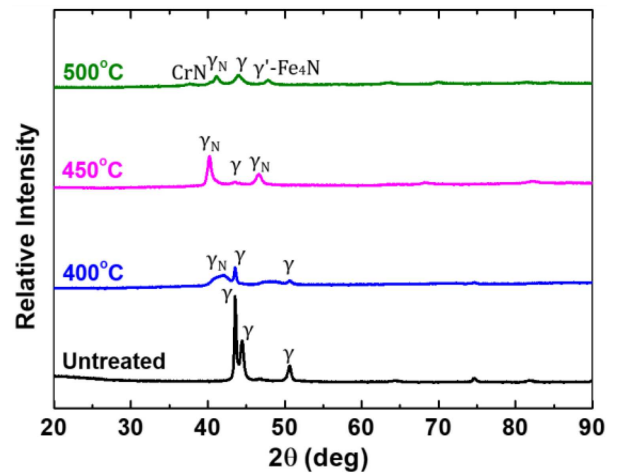


Fig. 3. X-ray diffraction of the untreated and plasma ion nitrided STS 304 specimen.

Figure 4 shows optical observation after cavitation-erosion test. The rough surface of the plasma ion nitrided specimen was found to be rough compared to the untreated material. The rough surface at untreated material was observed caused by the cavity impact, and the pit damage was observed by the continuous impact pressure at 10 h. In particular, the least damage morphology was observed at 450 °C, but the damage was increased at 500 °C. As a result of the surface observation, the cavitation-erosion resistance is improved after plasma ion nitriding at all the temperature conditions.

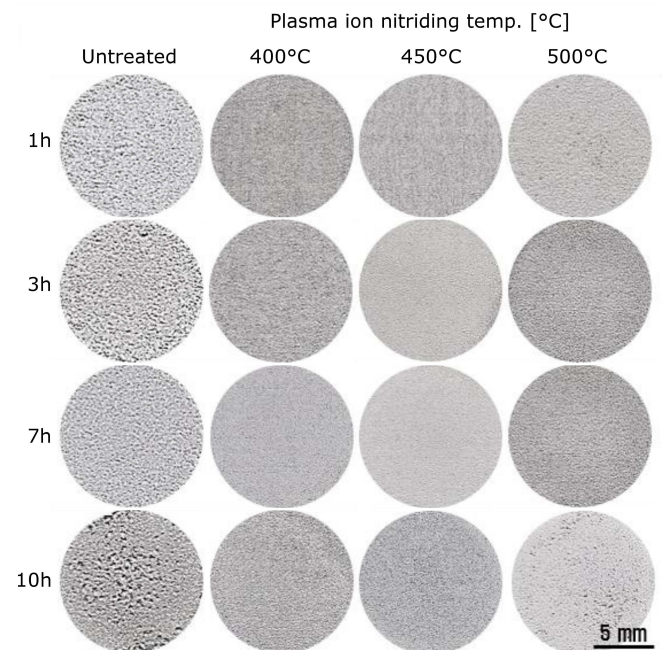


Fig. 4. Optical observation after cavitation-erosion test of the untreated and plasma ion nitrided STS 304 specimen.

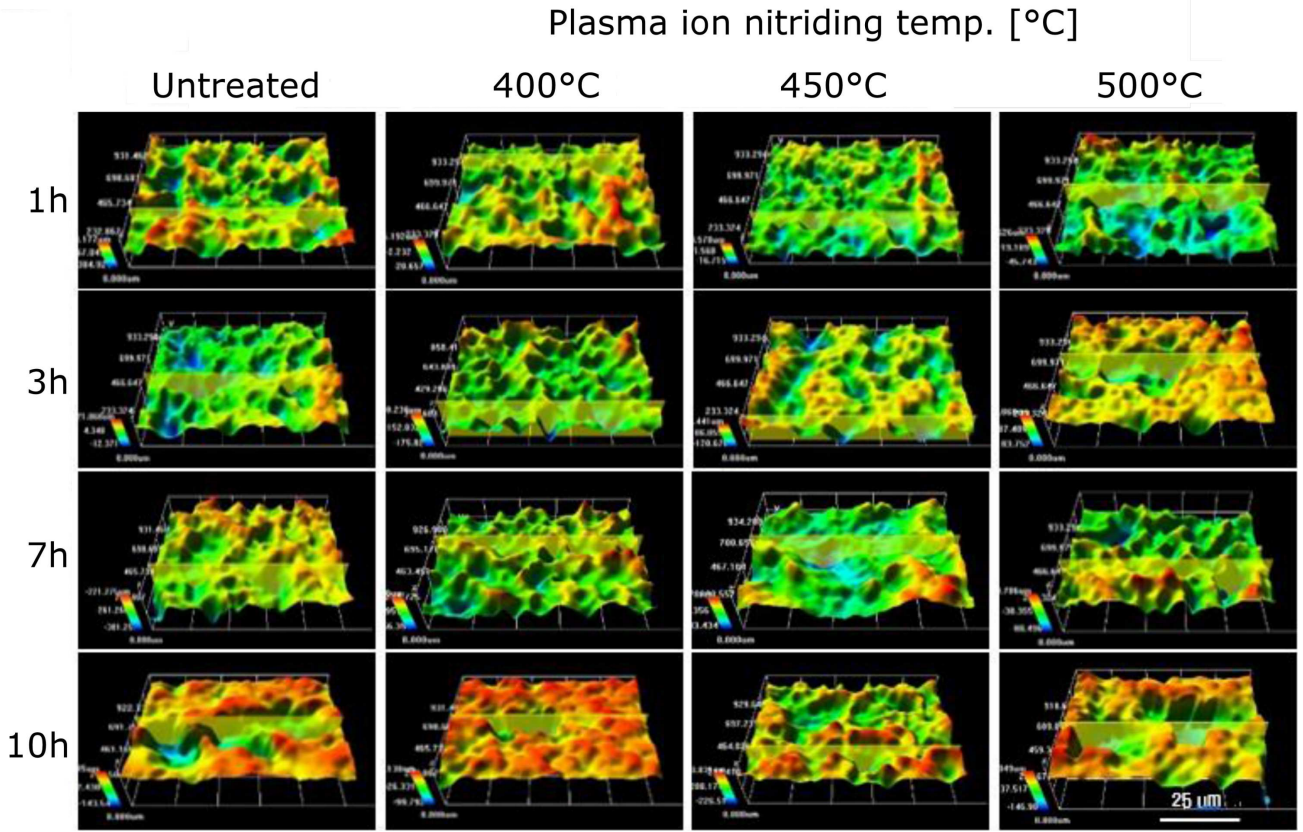


Fig. 5. 3D morphologies of the untreated and plasma ion nitrided STS 304 specimen after cavitation-erosion test.

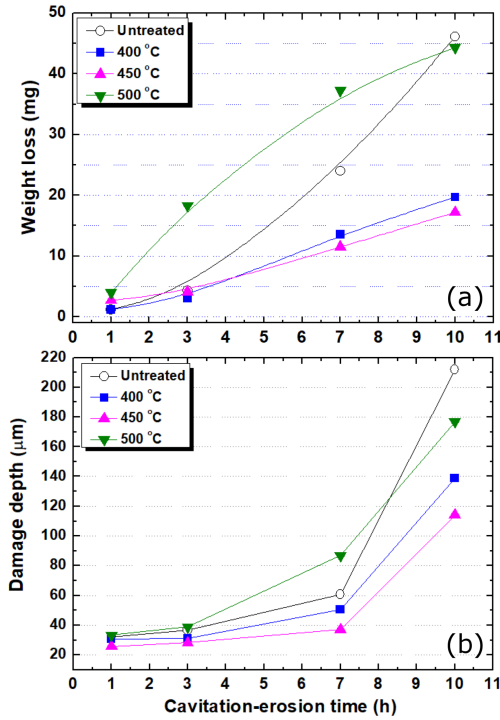


Fig. 6. Measurement after cavitation-erosion test of the untreated and plasma ion nitrided STS 304 specimen (a) weight loss, (b) damage depth.

The 3D microscope analysis after the cavitation-erosion experiment represented in Fig. 5. In overall, the cavity impact and micro-jet were forced to the rough material surface, and the rough surface irregularities was flattened by the continuous micro-jet. Furthermore, local damage occurred in the relatively weak part of the material surface and the impulse energy accumulated and the damage increased. Especially under seawater environment, micro galvanic corrosion occurs due to the difference of compressive residual stresses between the local damage region and non-damaged region, accelerating the damage by electrochemical reaction [15].

Figure 6 depicts the weight loss (Fig. 6a) and damage depth (Fig. 6b) after cavitation-erosion experiments. Cavitation-erosion experiment at 10 h, less damage depth in all plasma ion nitriding specimens was observed than that of the untreated material due to the formation of γ_N phase. The lowest weight loss and depth of damage at 450 °C, which is the deepest and most abundant γ_N phase, were shown. On the other hand, at 500 °C, brittle behavior due to the increase of internal residual stress by the formation of γ' -Fe₄N phase and electrochemical corrosion caused by chloride ion in the seawater resulted in increased damage. However, less cavitation-erosion damage was measured than untreated material due to the γ_N phase.

4. Conclusion

Cavitation-erosion damage behavior of STS 304 in seawater solution was analyzed after plasma nitridation at 400–500 °C. The γ_N phase, which improves the corrosion resistance at all process temperatures, was represented and the hardness was increased accordingly. In particular, the greatest thickness γ_N phase was formed at 450 °C, and a significant high hardness value was measured at 500 °C due to the formation of CrN and γ' -Fe₄N phases. Cavitation-erosion experiments for 10 h at 450 °C showed the least surface damage, weight loss and damage depth due to the formation of γ_N phase. On the other hand, less damage behavior at 500 °C showed than that of the untreated material due to the γ_N phase, but the damage tends to increase due to the brittle behavior by CrN and γ' -Fe₄N phases.

Acknowledgments

This research was supported by Defense Agency for Technology and Quality, Korea. This research was a part of the project titled “Construction of eco-friendly Al ship with painting, and maintenance/repairment free” funded by the Ministry of Oceans and Fisheries, Korea.

References

- [1] A.J. Sedriks, *Corrosion of Stainless Steels*, 2nd ed., Wiley-Interscience, New York 1996.
- [2] M. Divakar, V.K. Agarwal, S.N. Singh, *Wear* **259**, 110 (2005).
- [3] M. Samandi, B.A. Shedden, D.I. Smith, G.A. Collins, R. Hutchings, J. Tendys, *Surf. Coat. Technol.* **59**, 261 (1993).
- [4] L.A. Espitia, L. Varela, C.E. Pinedo, A.P. Tschiptschin, *Wear* **301**, 449 (2013).
- [5] S.O. Chong, S.J. Kim, *Jpn. J. Appl. Phys.* **56**, 01AG03 (2017).
- [6] L.A. Espitia, L. Varela, C.E. Pinedo, A.P. Tschiptschin, *Wear* **301**, 449 (2013).
- [7] A.N. Allenstein, C.M. Lepienski, A.J.A. Buschinelli, S.F. Brunatto, *Wear* **309**, 159 (2014).
- [8] P. Gallagher, R.E. Malpas, E.B. Shone, *Br. Corros. J.* **23**, 229 (1988).
- [9] S.O. Chong, S.J. Kim, *Jpn. J. Appl. Phys.* **56**, 01AC04 (2017).
- [10] *ASTM G32-06, Standard Test Method for Cavitation Erosion Using Vibratory Apparatus*, ASTM International, West Conshohocken (PA) 2006.
- [11] H. Michel, T. Czerwiec, M. Gantois, D. Ablitzer, A. Ricard, *Surf. Coat. Technol.* **72**, 103 (1995).
- [12] E. Menthe, K.T. Rie, J.W. Schultze, S. Simson, *Surf. Coat. Technol.* **74**, 412 (1995).
- [13] L. Nosei, S. Farina, M. Avalos, L. Nachez, B.J. Gomez, J. Feugeas, *Thin Solid Films* **516**, 1044 (2008).
- [14] S.O. Chong, S.J. Kim, *J. Kor. Inst. Surf. Eng.* **50**, 91 (2017).
- [15] D.A. Jones, *Principles and Prevention of Corrosion*, 2nd ed., Prentice Hall, New Jersey 1996.